

A long-lived lunar dynamo driven by continuous mechanical stirring

C. A. Dwyer¹, D. J. Stevenson² & F. Nimmo¹

Lunar rocks contain a record of an ancient magnetic field that seems to have persisted for more than 400 million years^{1,2} and which has been attributed to a lunar dynamo^{3,4}. Models of conventional dynamos driven by thermal or compositional convection have had difficulty reproducing the existence and apparently long duration of the lunar dynamo^{5–7}. Here we investigate an alternative mechanism of dynamo generation: continuous mechanical stirring arising from the differential motion, due to Earth-driven precession of the lunar spin axis, between the solid silicate mantle and the liquid core beneath^{8,9}. We show that the fluid motions and the power required to drive a dynamo operating continuously for more than one billion years and generating a magnetic field that had an intensity of more than one microtesla 4.2 billion years ago³ are readily obtained by mechanical stirring. The magnetic field is predicted to decrease with time and to shut off naturally when the Moon recedes far enough from Earth that the dissipated power is insufficient to drive a dynamo; in our nominal model, this occurred at about 48 Earth radii (2.7 billion years ago). Thus, lunar palaeomagnetic measurements may be able to constrain the poorly known early orbital evolution of the Moon. This mechanism may also be applicable to dynamos in other bodies, such as large asteroids.

Several lines of evidence^{2,10} point to the Moon having an iron core that is 300–400 km in radius and probably at least partly molten at the present day. A recent palaeomagnetic study³ has strengthened the case that the observed lunar magnetic anomalies are due to an ancient dynamo⁴ rather than an external source such as impacts¹¹. Although deriving palaeointensities from lunar samples is difficult^{2,12}, the results of ref. 3 raise the question of how a lunar dynamo could be maintained.

Dynamos are usually assumed to arise as a result of thermal or compositional convection driven by removal of heat into the overlying mantle¹³. A long-lived, convection-driven lunar dynamo is difficult to sustain because it requires rapid core cooling. The lunar mantle is unlikely to permit persistent rapid cooling, unless special conditions are invoked^{5–7}.

Shortly after the Moon's formation, when the Earth–Moon distance was <26–29 Earth radii (R_e), the lunar core precessed with the mantle^{14,15}, but as the distance increased, differential motion between core and mantle is predicted to have occurred because the core and the mantle precess around slightly different axes^{8,9,14,15} (Fig. 1, inset). The essential idea in our model is that this leads to turbulent motions in the core with amplitudes of the order of the core–mantle differential velocity. These motions are of sufficient amplitude to produce a magnetic Reynolds number of $\sim 10^4$ or more, which is a necessary but not sufficient condition for a dynamo (Supplementary Information, section 2). Our analysis is consistent with ref. 16, where it was shown that differential motion can drive a dynamo under some conditions; and in Supplementary Information, section 2, we argue that the early lunar core satisfies these conditions.

The turbulent friction from the differential motion at the core–mantle boundary (CMB), results in a small departure of the Moon's rotation axis from the plane defined by the lines perpendicular to the ecliptic and the plane of the lunar orbit^{8,9}. The power dissipated at this

boundary at the present day is $(6.0 \pm 1.6) \times 10^7$ W (ref. 9). In the weak (low-viscosity) limit, in which core–mantle coupling is small, the power varies as $n^3 \sin^3(I_e)$ (ref. 9), where n is the mean motion of the lunar orbit and I_e (the equatorial inclination) is the angle between the lunar spin axis and the ecliptic normal (Fig. 1, inset).

The power available to produce a magnetic field depends on how both n (or equivalently, the semimajor axis of the lunar orbit, a) and I_e have varied over time (Methods). Because the Moon is in a Cassini state¹⁷, the lunar semimajor axis and equatorial inclination are related¹⁸. At early times, when the Moon was closer to Earth, the equatorial inclination was larger (Supplementary Fig. 1). The Moon

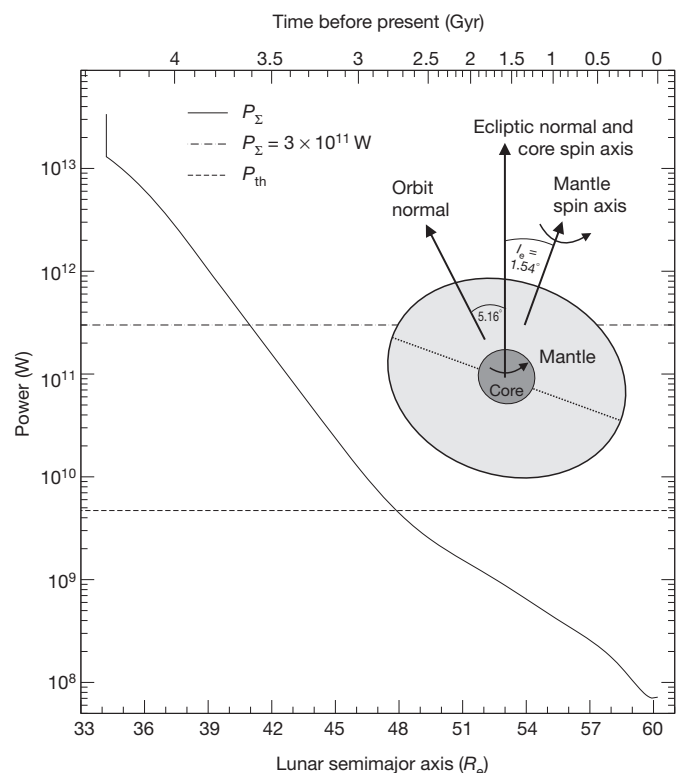


Figure 1 | The total power deposited into the lunar core. The solid line shows the total power deposited into the lunar core, P_Σ , as a function of semimajor axis (equation (1); lower x axis). The adiabatic threshold value is marked P_{th} (dashed line). The dash-dot line is at $P_\Sigma = 3 \times 10^{11}$ W (see text). The time before present is plotted at the top, calculated using the results of ref. 20 (Methods). There are 7×10^{28} J of energy available for dynamo generation between the time of the Cassini-state transition and the cessation of the dynamo (using our nominal evolution model). The inset shows the geometry of the situation. The mean motion, n , of an orbit is related to the semimajor axis, a , through $n = (GM_e/a^3)^{0.5}$, where M_e is the mass of Earth. For the purposes of display, the calculations were performed with no truncation of coefficients.

¹Department of Earth and Planetary Sciences, University of California Santa Cruz, 1156 High Street, Santa Cruz, California 95064, USA. ²Division of Geologic and Planetary Sciences, California Institute of Technology, Pasadena, California 91125, USA.

probably also underwent a transition in the Cassini state it was in at $a \approx 34R_e$ (ref. 18).

The temporal evolution of the lunar orbit is poorly constrained at times before 600 million years (0.6 Gyr) ago¹⁹. Here we have used the results of ref. 20 to relate the lunar semimajor axis to the time before present (Methods and Supplementary Figs 1 and 2); we discuss details and how the use of other models would affect our results in Supplementary Information, section 3. On the basis of the measured present-day dissipation rate⁹, the total power dissipated at the lunar CMB, P_{Σ} , at time t is given by

$$P_{\Sigma}(t) = \left(\frac{a(t_n)}{a(t)}\right)^{9/2} \left(\frac{\sin[I_e(t)]}{\sin[I_e(t_n)]}\right)^3 P_{\Sigma}(t_n) \quad (1)$$

$$\approx 3 \times 10^{20} \text{ W} \times \frac{\sin^3[I_e(t)]}{(a(t)/R_e)^{9/2}}$$

where t_n denotes the time at the present day and $I_e(t_n) = 1.54^\circ$.

Not all of the power dissipated at the CMB is available to generate a dynamo; thus, there is a threshold power, P_{th} , at which the dynamo will cease. The power available to generate a dynamo is

$$P_{\text{dyn}} = P_{\Sigma} - P_{\text{th}} \quad (2)$$

However, the value of P_{th} is poorly constrained. The maximum value P_{th} could have is that required to maintain a completely liquid core in a well-mixed, adiabatic state¹³, for which $P_{\text{th}} = 4.7 \times 10^9 \text{ W}$ (Supplementary Table 1). It is likely that the correct value is smaller than this for two reasons: the presence of a growing inner core¹⁰ would reduce the power needed to maintain an adiabat; and under some conditions, through-going fluid motions can occur in a subadiabatic fluid if the outer boundary surface is ellipsoidal²¹. Therefore, our use of the adiabatic value as P_{th} is conservative, in that it will result in a minimum-duration estimation of the dynamo lifetime and underestimation of field intensity at a given Earth–Moon distance.

Figure 1 shows the evolution of the power dissipated at the CMB, P_{Σ} , compared with P_{th} . The power dissipated decreases rapidly with time as the semimajor axis increases and drops below the adiabatic threshold at $a \approx 48R_e$. In our nominal evolution model, this occurs 2.7 Gyr ago, but other temporal models would result in different threshold times (Supplementary Information, section 3), as would using different threshold values.

We estimate the magnetic field on the basis of the available power. This approach neglects the spatial pattern of the flow, which may be important^{16,22} and will require future work. There need be no simple connection between palaeointensity and available power because the dissipation can be on smaller scales than the large-scale current, but it is nonetheless useful to consider possible scalings for the field. For our first model (model A), we will derive a scaling for the lunar palaeofield based on Earth's current magnetic field (Methods):

$$B_{\text{Am}}(t) = B_e(t_n) \frac{R_e^3}{R_m^3} \left(\frac{R_{\text{cm}}}{R_{\text{ce}}}\right)^{5/2} \left(\frac{P_{\text{dyn,m}}(t)}{P_{\text{dyn,e}}(t_n)}\right)^{1/2} \quad (3)$$

$$\approx 1 \mu\text{T} \times \left(\frac{P_{\text{dyn,m}}(t)}{3 \times 10^{11} \text{ W}}\right)^{1/2}$$

Here R_{cm} and R_{ce} are the radii of the Moon and Earth's cores, R_m is the radius of the Moon, $P_{\text{dyn,m}}$ and $P_{\text{dyn,e}}$ are the respective powers available to drive a dynamo for the Moon and Earth, B_e is the terrestrial surface magnetic field strength and B_{Am} is the lunar surface magnetic field strength predicted by model A.

The numerical value in equation (3) was derived by using the values given in Supplementary Table 1. The largest source of uncertainty is in the value of the available power for Earth's core, $P_{\text{dyn,e}}$. Here we have taken $P_{\text{dyn,e}} = 10^{13} \text{ W}$ (ref. 13), which will result in a conservatively small lunar field strength (Supplementary Information, section 1).

For our second model (model B), we use a set of model results and direct scalings from ref. 23. We obtain

$$B_{\text{Bm}} \approx d \left(\frac{R_{\text{cm}}}{R_m}\right)^3 (2\mu_0 c f_{\text{ohm}} \rho_c)^{1/2} \left(\frac{\alpha_c G}{3C_{p,c}}\right)^{1/3} P_{\text{dyn,m}}^{1/3} \quad (4)$$

$$\approx 6d \mu\text{T} \times \left[\frac{P_{\text{dyn,m}}(t)}{3 \times 10^{11} \text{ W}}\right]^{1/3}$$

where d is the ratio of the dipolar magnetic field to the total field at the CMB, μ_0 is the magnetic permeability in vacuum, f_{ohm} is the ratio of ohmic dissipation to total dissipation, ρ_c is the density of the core, α_c is the coefficient of linear thermal expansion of the core and $C_{p,c}$ is the heat capacity of the core (see Methods and Supplementary Table 1 for symbol values). Figure 2 shows how the surface field strengths based on our two different scalings (equations (3) and (4)) evolve with time. For model B, we show two curves, one with $d = 1$ and one with $d = 1/7$ (Methods and Supplementary Fig. 3). For both models, the predicted field strength decreases to zero once the available power is less than the threshold value ($a \approx 48R_e$, $t \approx 2.7$ Gyr ago). The field strengths decrease as the Moon moves outward, but at different rates. At 4 Gyr ago, the predicted field strengths are in the range ~ 1 – $10 \mu\text{T}$. According to ref. 16, the surface field is expected to be dominantly dipolar and to undergo periodic reversals. However, because of predicted variations in pole orientation¹⁶ and likely impact-induced reorientation²⁴, existing inferences of magnetic palaeopole orientations based on remote sensing data⁴ do not provide a strong observational constraint on our model.

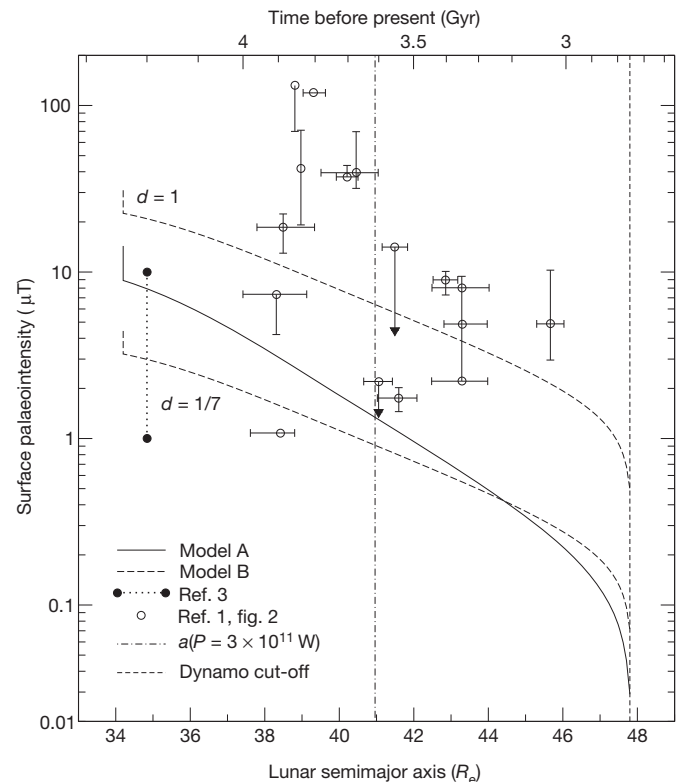


Figure 2 | The lunar surface magnetic palaeointensity predicted by our models. Model A (equation (3)) is shown by the solid line and model B (equation (4)) is shown by the (non-vertical) dashed lines; for model B, two lines are shown, with respective ratios of dipolar field strength to total field strength of $d = 1$ and $1/7$, as shown. The estimate range of ref. 3 is plotted as filled circles. Older palaeointensity data and error bars (from fig. 2 in ref. 1) are plotted as open circles. The vertical dash-dot line indicates the distance at which the power dissipated is exactly $3 \times 10^{11} \text{ W}$, and the vertical dashed line denotes the minimum cut-off age of the dynamo (see text). For the purposes of display, the calculations were performed with no truncation of coefficients. The error bars are defined in ref. 1 as follows: “horizontal error bars reflect the published uncertainty values associated with the radiometric age determinations. Vertical error bars reflect variations in intensity between subsamples ... [and] uncertainties in the fit between the data and lines correspond to various palaeofields”.

A recent estimate of lunar palaeointensity³ gives a value of $\sim 1\text{--}10\ \mu\text{T}$ at 4.2 Gyr ago (Fig. 2). This range is compatible with our models. Older palaeointensity estimates¹ for 3.0–4.0 Gyr ago are also plotted in Fig. 2, although these are probably less reliable^{2,12}. Many of the palaeointensities fall within our model range, although the high values corresponding to $\sim 3.6\text{--}3.9$ Gyr ago might require an additional driving mechanism^{11,25} or a smaller P_{th} . Nonetheless, our results suggest that a mechanically driven dynamo could persist for at least ~ 1.6 Gyr, which is much longer than any likely convection-driven dynamo.

Whereas the relationship between magnetic field intensity and lunar semimajor axis, a , is probably robust, the conversion of a to time is much more uncertain. For instance, although in our nominal model²⁰ $a = 48R_{\text{e}}$ occurs ~ 2.7 Gyr ago, in other models this distance might not occur until ~ 1.8 Gyr ago^{19,20,26,27} (Supplementary Information, section 3). Thus, our assessment of a billion-year lifetime for a mechanically stirred dynamo is probably conservative.

The simple relationship between dissipation and equatorial inclination shown in equation (1) is probably inappropriate at the earliest times. Stronger core–mantle coupling reduces the differential motion^{9,15,17}. Even when this coupling is weak, dissipation is probably self-limiting to $\sim 3 \times 10^{11}$ W because the overlying mantle will melt. At this dissipation rate, the core temperature increase over 0.1 Gyr (approximating the initial orbital evolution timescale) is about 1,000 K, which is enough to initiate mantle melting and reduce the effectiveness of core stirring.

Despite these caveats, however, our results raise several interesting possibilities. First, the model predicts a long-lived magnetic field that weakens with time, followed by an abrupt shut-off (Fig. 2). Thus, the palaeomagnetic record may ultimately be used to constrain the outward evolution of the Moon (and the dissipation rate within the Hadean Earth²⁸). Second, at the earliest distances ($a < 26R_{\text{e}}\text{--}29R_{\text{e}}$), when there is no differential motion¹⁵, our proposed mechanism does not generate a magnetic field. Therefore, we predict that rocks from this time period (according to our nominal model, this distance corresponds to before 4.45 Gyr ago) should be unmagnetized, unless other mechanisms were available^{11,25}. Third, similar mechanically driven dynamos may have operated in other bodies where tidally driven differential core–mantle motion may have occurred, such as large asteroids like 4 Vesta or the angrite parent body^{29,30}. Finally, our work also poses a challenge to numerical modellers of dynamos, namely that of determining the properties of mechanically driven dynamos.

METHODS SUMMARY

The relation between I_{e} and a . We fit the following explicit polynomial function (Supplementary Fig. 1) to the plot of obliquity versus semimajor axis, a (fig. 2 in ref. 18), using I_{e} = obliquity $- 5.16^{\circ}$:

$$I_{\text{e}}(a) = \begin{cases} 71.84^{\circ}; a = 34.2R_{\text{e}} \\ 0.1075^{\circ} \times \tilde{a}^{10} - 0.0332^{\circ} \times \tilde{a}^9 - 1.0008^{\circ} \times \tilde{a}^8 \\ + 0.6110^{\circ} \times \tilde{a}^7 + 2.7016^{\circ} \times \tilde{a}^6 - 1.7281^{\circ} \times \tilde{a}^5 \\ - 2.3280^{\circ} \times \tilde{a}^4 - 1.4509^{\circ} \times \tilde{a}^3 + 6.9951^{\circ} \times \tilde{a}^2 \\ - 6.6208^{\circ} \times \tilde{a} + 5.5828^{\circ}; 34.2R_{\text{e}} \leq a \leq 60.2R_{\text{e}} \end{cases} \quad (5)$$

where $\tilde{a} = (a/R_{\text{e}} - 46.6308)/7.7288$.

Palaeointensity models. Full derivations of these models may be found in Methods.

In model A (equation (3)), we assume that we can, using appropriate parameters, scale Earth's magnetic field to the Moon. We assume that the magnetic field at the surface of the Moon can be approximated as a current loop in the core with the following characteristics: the radius of the current loop is proportional to the radius of the core and the cross-sectional area of the current loop is proportional to the squared radius of the core. We assume that Earth's field can be similarly characterized. This is not intended as anything more than a rough guide to what is possible. In reality, it is probable that much of the dissipation associated with Earth's field occurs on scales far smaller than the largest current loop that could fit within Earth's core. Nevertheless, it tells us what field to expect in the (unlikely) case of similarity of Earth and the Moon's dynamos.

In model B (equation (4)), rather than scaling from Earth we use a set of model results and direct scalings from ref. 23. We used their equation (2) to estimate the field intensity at the top of the CMB. We set the efficiency factor to be

$F \approx 4\pi G \mu_0 \rho_{\text{c}} R_{\text{cm}}^2 / 3C_{\text{P,C}}$, scaled the field from the CMB to the surface by including a factor of $(R_{\text{cm}}/R_{\text{m}})^3$, and scaled the dipolar to total field strength at the CMB using the parameter d .

Full Methods and any associated references are available in the online version of the paper at www.nature.com/nature.

Received 17 May; accepted 15 September 2011.

- Cisowski, S. M., Collinson, D. W., Runcorn, S. K. & Stephenson, A. A review of lunar paleointensity data and implications for the origin of lunar magnetism. *J. Geophys. Res.* **88**, A691–A704 (1983).
- Wieczorek, M. A. *et al.* in *New Views of the Moon* (eds Jolliff, B. L., Wieczorek, M. A., Shearer, C. K. & Neal, C. R.) 60, 221–364 (Mineralogical Society of America, 2006).
- Garrick-Bethell, I., Weiss, B. P., Shuster, D. L. & Buz, J. Early lunar magnetism. *Science* **323**, 356–359 (2009).
- Hood, L. L. Central magnetic anomalies of Nectarian-aged lunar impact basins: probable evidence for an early core dynamo. *Icarus* **211**, 1109–1128 (2011).
- Stegman, D. R., Jellinek, A. M., Zatman, S. A., Baumgardner, J. R. & Richards, M. A. An early lunar core dynamo driven by thermochemical mantle convection. *Nature* **421**, 143–146 (2003).
- Takahashi, F. & Tsunakawa, H. Thermal core-mantle coupling in an early lunar dynamo: implications for a global magnetic field and magnetosphere of the early Moon. *Geophys. Res. Lett.* **36**, L24202 (2009).
- Konrad, W. & Spohn, T. Thermal history of the Moon: implications for an early core dynamo and post-accretional magmatism. *Adv. Space Res.* **19**, 1511–1521 (1997).
- Yoder, C. F. The free librations of a dissipative Moon. *Phil. Trans. R. Soc. Lond. A* **303**, 327–338 (1981).
- Williams, J. G., Boggs, D. H., Yoder, C. F., Ratcliff, J. T. & Dickey, J. O. Lunar rotational dissipation in solid body and molten core. *J. Geophys. Res.* **106**, 27933–27968 (2001).
- Weber, R. C., Lin, P.-Y., Garnero, E. J., Williams, Q. & Lognonné, P. Seismic detection of the lunar core. *Science* **331**, 309–312 (2011).
- Hood, L. L. & Artemieva, N. A. Antipodal effects of lunar basin-forming impacts: initial 3D simulations and comparisons with observations. *Icarus* **193**, 485–502 (2008).
- Lawrence, K., Johnson, C., Tauxe, L. & Gee, J. Lunar paleointensity measurements: implications for lunar magnetic evolution. *Phys. Earth Planet. Inter.* **168**, 71–87 (2008).
- Nimmo, F. in *Core Dynamics* (ed. Olson, P.) 31–65 (Treatise on Geophysics 8, Academic, 2007).
- Goldreich, P. Precession of the Moon's core. *J. Geophys. Res.* **72**, 3135–3137 (1967).
- Meyer, J. & Wisdom, J. Precession of the lunar core. *Icarus* **211**, 921–924 (2011).
- Tilgner, A. Precession-driven dynamos. *Phys. Fluids* **17**, 034104 (2005).
- Peale, S. J. Generalized Cassini's laws. *Astron. J.* **74**, 483–489 (1968).
- Ward, W. R. Past orientation of the lunar spin axis. *Science* **189**, 377–379 (1975).
- Williams, G. E. Geological constraints on the Precambrian history of Earth's rotation and the Moon's orbit. *Rev. Geophys.* **38**, 37–59 (2000).
- Webb, D. J. Tides and the evolution of the Earth-Moon system. *Geophys. J. R. Astron. Soc.* **70**, 261–271 (1982).
- Cébron, D., Maubert, P. & Le Bars, M. Tidal instability in a rotating and differentially heated ellipsoidal shell. *Geophys. J. Int.* **182**, 1311–1318 (2010).
- Roberts, P. H., Glatzmaier, G. A. & Clune, T. L. Numerical simulation of a spherical dynamo excited by a flow of von Karman type. *Geophys. Astrophys. Fluid Dyn.* **104**, 207–220 (2010).
- Christensen, U. R., Holzwarth, V. & Reiners, A. Energy flux determines magnetic field strength of planets and stars. *Nature* **457**, 167–169 (2009).
- Ong, L. & Melosh, H. J. in *41st Lunar Planet. Sci. Conf.* abstr. 1363, (<http://www.lpi.usra.edu/meetings/lpsc2010/pdf/1363.pdf>) (Lunar and Planetary Institute, 2010).
- Le Bars, M., Wieczorek, M. A., Karatekin, Ö., Cébron, D. & Laneuville, M. An impact-driven dynamo for the early Moon. *Nature* (<http://dx.doi.org/10.1038/nature10565>) (this issue).
- Ooe, M., Sasaki, H. & Kinoshita, H. in *Variations in Earth Rotation* (eds McCarthy D. D. & Carter, W. E.) 51–57 (American Geophysical Union, 1990).
- Walker, J. C. G. *et al.* in *Earth's Earliest Biosphere* (ed. Schopf, J.) 260–290 (Princeton Univ. Press, 1983).
- Zahnle, K. *et al.* Emergence of a habitable planet. *Space Sci. Rev.* **129**, 35–78 (2007).
- Weiss, B. P. *et al.* Magnetism on the angrite parent body and the early differentiation of planetesimals. *Science* **322**, 713–716 (2008).
- Bills, B. G. & Nimmo, F. Forced obliquities and moments of inertia of Ceres and Vesta. *Icarus* **213**, 496–509 (2011).

Supplementary Information is linked to the online version of the paper at www.nature.com/nature.

Acknowledgements C.A.D. would like to thank B. P. Weiss and I. Garrick-Bethell for discussions.

Author Contributions D.J.S. thought of the initial idea. C.A.D. performed the calculations. F.N. investigated the conditions under which turbulence occurs. All authors discussed the results and implications and commented on the manuscript.

Author Information Reprints and permissions information is available at www.nature.com/reprints. The authors declare no competing financial interests. Readers are welcome to comment on the online version of this article at www.nature.com/nature. Correspondence and requests for materials should be addressed to C.A.D. (cadwyer@ucsc.edu).

METHODS

The relation between I_c and a . The Moon is presently in a Cassini state and has been since at least¹⁸ the time at which $a = 34.2R_e$. Thus, there is a functional relationship between I_c and a over the range of a between that time and the present day. The relationship between I_c and a as determined by ref. 18 was numerical. We arrived at an explicit expression for I_c in the following way. We digitized the plot shown in fig. 2 of ref. 18 over the range of interest, converted obliquity to I_c (using $I_c = \text{obliquity} - 5.16^\circ$), smoothed the line and then fitted a tenth-order polynomial:

$$I_c(a) = \left\{ \begin{array}{l} 71.84^\circ; a = 34.2R_e \\ 0.1075^\circ \times \tilde{a}^{10} - 0.0332^\circ \times \tilde{a}^9 - 1.0008^\circ \times \tilde{a}^8 \\ + 0.6110^\circ \times \tilde{a}^7 + 2.7016^\circ \times \tilde{a}^6 - 1.7281^\circ \times \tilde{a}^5 \\ - 2.3280^\circ \times \tilde{a}^4 - 1.4509^\circ \times \tilde{a}^3 + 6.9951^\circ \times \tilde{a}^2 \\ - 6.6208^\circ \times \tilde{a} + 5.5828^\circ; 34.2R_e \leq a \leq 60.2R_e \end{array} \right\} \quad (5)$$

where $\tilde{a} = (a/R_e - 46.6308)/7.7288$. In Supplementary Fig. 1, we have plotted I_c and a against time before present (t), with the relationship between a and t calculated using the model described in the next section. Equation (5) is only an approximation to the relationship in ref. 18; however, given the great uncertainty in the a -to- t relation (Supplementary Information, section 3.1), the errors introduced by the use of equation (5) are not important. Likewise, errors in the result of ref. 18 are likely to be negligible in comparison with the uncertainties in the relation between a and t .

Converting a into time before present (t). As Cassini-state theory does not include time, a separate, independent relationship for the temporal evolution of the lunar orbit must be assumed. There is extreme uncertainty in this over the distances and times of interest, resulting in great temporal variability in any model (Supplementary Information, section 3). In addition to our nominal model (described below), we also examined four other possible models. We compare these models in Supplementary Information (section 3.2 therein and Supplementary Figs 2 and 3). We require that models for the lunar orbit fit the available geologic constraints¹⁹ and we assume that the Moon formed at about the Roche limit²¹ some time shortly after the Solar System formed.

The nominal model of this paper was modified from models c and d of ref. 20. Model c included only power dissipation from an ocean and model d included power dissipation in both the ocean and solid Earth. Neither model predicted lunar formation at ~ 4.6 Gyr ago, but the two predicted formation ages bracketed that value.

We digitized (a, t) points for both these models and used a weighted average to combine them into an evolution model in which the Moon formed 4.6 Gyr ago. The weighted mean was calculated in the following manner: the (a, t) curves were interpolated to have a common point spacing, and a weighted average of the t values at each a point was taken to derive the final (a, t) model. The weights were determined by applying the lever rule to the goal formation age (4.6 Gyr ago) and the curves' respective formation ages. This model is plotted in Supplementary Figs 1 and 2.

Palaeointensity models. We make the simplifying assumption that we may relate the surface magnetic field strength to the power available to the lunar dynamo. We consider two separate models for lunar palaeointensity: models A and B.

In model A (equation (3)), we assume that we can, using appropriate parameters, scale Earth's magnetic field to the Moon. We assume that the magnetic field at the surface of the Moon can be approximated as a current loop in the core with the following characteristics: the radius of the current loop is proportional to the radius of the core and the cross-sectional area of the current loop is proportional to the squared radius of the core. We assume that Earth's field can be similarly characterized. This is not intended as anything more than a rough guide to what is possible. In reality, it is probable that much of the dissipation associated with Earth's field occurs on scales far smaller than the largest current loop that could fit within Earth's core. Nevertheless, it tells us what field to expect in the (unlikely) case of similarity of Earth and the Moon's dynamos.

What follows is the derivation of the expression for the lunar surface palaeointensity as a function of available power (that is, equation (3) of the main text):

From electromagnetism it follows that

$$P = I^2 R_s$$

where P denotes power, I denotes current and R_s denotes resistance. Also, the intensity of a magnetic field is

$$B = \mu_0 I R_1^2 / 2D^3$$

where D is the distance between the centre of the current loop and the point where the field is measured and R_1 is the radius of the current loop. The resistance is

$$R_s = L/\sigma A_c$$

where σ denotes conductivity, L is the length of the current loop and A_c is the cross-sectional area of the current loop.

Combining the above, we have

$$B = \frac{\mu_0 R_1^2}{2D^3} \left(\frac{P\sigma A_c}{L} \right)^{1/2}$$

Because we are interested in the strengths of fields on the surface of the planet, $D = R_p$. Additionally, we assume that the following proportionalities hold: $L \propto R_c$, $R_1 \propto R_c$, $A_c \propto R_c^2$ (where R_c is the radius of the planet's core). This gives

$$B \propto \frac{P^{1/2} R_c^{5/2}}{R_p^3}$$

We can determine the constant of proportionality using Earth's present-day field.

Thus, with t_n denoting the present day, the palaeointensity of the lunar surface field as predicted by our model A is given by equation (3):

$$\begin{aligned} B_{Am}(t) &= B_c(t_n) \frac{R_c^3}{R_m^3} \left(\frac{R_{cm}}{R_{ce}} \right)^{5/2} \left(\frac{P_{dyn,m}(t)}{P_{dyn,c}(t_n)} \right)^{1/2} \\ &\approx 1\mu\text{T} \times \left(\frac{P_{dyn,m}(t)}{3 \times 10^{11}\text{W}} \right)^{1/2} \end{aligned}$$

In model B, rather than scaling from Earth we use a set of model results and direct scalings from ref. 23. According to equation (2) of ref. 23

$$\langle B \rangle^2 (2\mu_0)^{-1} = c f_{ohm} \langle \rho_c \rangle^{1/3} (F q_0)^{2/3}$$

Here B is the magnetic field strength within the dynamo; μ_0 is the permeability of free space; $q_0 = (P_\Sigma - P_{ad})(4\pi R_{cm}^2)^{-1}$ is the heat flux at the CMB in excess of the adiabatic value (see Supplementary Information of ref. 23); c , f_{ohm} and F are constants; and angle brackets denote averages over the volume over which the kinetic energy (from the differential rotation, in this case) is added to the core. The values of c and f_{ohm} given in Supplementary Table 1 are taken directly from ref. 23.

F is defined in equation (3) of ref. 23 as

$$F^{2/3} = \frac{1}{\text{Vol}} \int_{r_a}^{r_b} \left(\frac{q_c(r)}{q_0} \frac{L(r)}{H_T(r)} \right)^{2/3} \left(\frac{\rho(r)}{\langle \rho \rangle} \right)^{1/3} 4\pi r^2 dr \quad (6)$$

where Vol is the volume described above; r_a and r_b are respectively the lower and upper radial bounds of the volume; $q_c(r)$ is the power per unit area as a function of radius; $L(r)$ is the length scale of the largest convective structure; $H_T(r) = C_p(\alpha g(r))^{-1}$ is the temperature scale height as a function of radius; C_p is the heat capacity; α is the coefficient of linear thermal expansion; and $g(r)$ is the acceleration due to gravity as a function of radius.

Because the magnetic field strength depends on the total power and not on the spatial distribution with which it is deposited²³, we simplify this equation by assuming that all the terms within the integral are constant, and derive the following expression for F :

$$F \approx \frac{4\pi G \alpha_c \rho_c R_{cm}^2}{3C_{p,c}} \quad (7)$$

Different assumptions (for example letting q_c vary linearly with r) yield results differing by a factor of order one.

We set the scale height of temperature to be $C_{p,c}(\alpha_c g_{cm})^{-1}$ and the scale height for convection to be R_{cm} , we set $g_{cm} = GM_{cm}R_{cm}^{-2} = 4\pi GR_{cm}\rho_c/3$, we take Vol to be the volume of the entire core and we approximate $\langle B \rangle$ by $B_m(R_{cm})$.

Because the lunar core has a small radius, only the dipolar part of the magnetic field is likely to be detectable at the surface. The magnetic field within the dynamo-generating region will contain higher-degree components^{16,23}. However, the ratio of the dipolar field strength to the total field strength at the CMB is somewhat uncertain, especially as precession-driven dynamos seem to have power spectra different from those of convective dynamos¹⁶. We have therefore defined a term, d , that is the ratio of the dipolar field strength to the total field strength at the top of the dynamo region (the CMB). For convection-driven dynamos²³, $d \approx 1/7$, and for the (probably unrealistic) purely dipolar case, $d = 1$. For $d < 1$, this correction has the result of reducing the predicted (dipolar) surface field strength (note that such a correction is not needed in model A). Taking this correction into account, the

lunar surface palaeointensity predicted by our model B is that given in equation (4):

$$B_{\text{Bm}} \approx d \left(\frac{R_{\text{cm}}}{R_{\text{m}}} \right)^3 (2\mu_0 c f_{\text{ohm}} \rho_c)^{1/2} \left(\frac{\alpha_c G}{3C_{p,c}} \right)^{1/3} P_{\text{dyn,m}}^{1/3}$$

$$\approx 6d \mu\text{T} \times \left[\frac{P_{\text{dyn,m}}(t)}{3 \times 10^{11} \text{ W}} \right]^{1/3}$$

Here the factor of $(R_{\text{cm}}/R_{\text{m}})^3$ scales the magnetic field strength from the CMB to the surface.

A further source of uncertainty in this model is in the calculation of the efficiency factor, F . Although this factor does depend on the spatial distribution of the power, it is the total power that really matters²³; thus, this uncertainty is unlikely to affect our conclusions significantly. An additional concern is the extent to which numerical models of terrestrial and stellar dynamos have the same scaling behaviour as mechanically driven dynamos of the kind we are proposing here (for example in the ratio of dipolar to higher-degree terms). We carry out a limited discussion of this topic in Supplementary Information, section 2, but further work will be needed.

31. Canup, R. M. & Asphaug, E. Origin of the Moon in a giant impact near the end of the Earth's formation. *Nature* **412**, 708–712 (2001).